Spin-ordering and magnetoelastic coupling in the extended kagome system $YBaCo_4O_7$

D. D. Khalyavin,[1] P. Manuel,[1] B. Ouladdiaf,[2] A. Huq,[3] P. W. Stephens,[4] H. Zheng,[3] J. F. Mitchell,[3] and L. C. Chapon[1]

[1]*ISIS facility, Rutherford Appleton Laboratory-CCLRC, Chilton, Didcot, Oxfordshire, OX11 0QX, United Kingdom*

[2]*Institute Laue-Langevin, 6 Rue Jules Horowitz, BP 156, F-38042 Grenoble Cedex 9, France*

[3]*Materials Science Division, Argonne National Laboratory, Argonne, Illinois 60439, USA*

[4]*Department of Physics and Astronomy, Stony Brook University, Stony Brook, New York 11794-3800*

(Received 27 July 2010; revised manuscript received 25 January 2011; published 15 March 2011; corrected 8 February 2012)

Low-temperature magnetic and structural behavior of the extended Kagome system $YBaCo_4O_7$ has been studied by single-crystal neutron diffraction and high-resolution powder x-ray diffraction. Long-range magnetic ordering associated with a structural transition from orthorhombic $Pbn2_1$ to monoclinic $P2_1$ symmetry has been found at $T_1 \sim 100$ K. The interplay between the structural and magnetic degrees of freedom indicates that the degeneracy of the magnetic ground state, present in the orthorhombic phase, is lifted through a strong magnetoelastic coupling, as observed in other frustrated systems. At $T_2 \sim 60$ K, an additional magnetic transition is observed, though isosymmetric. Models for the magnetic structures below T_1 and T_2 are presented, based on refinements using a large number of independent reflections. The results obtained are compared with previous single-crystal and powder-diffraction studies on this and related compositions.

DOI: 10.1103/PhysRevB.83.094412 PACS number(s): 75.25.−j, 75.85.+t, 61.05.F−

I. INTRODUCTION

The magnetic behavior of systems with competitive exchange interactions has been the focus of attention over the past several decades. This competition can arise from comparable strength between nearest- and beyond-nearest-neighbor interactions or due to specific symmetry of the exchange topology.[1] The latter, usually referred to as geometrical frustration, can be found in many materials where magnetic ions form a network of triangular-based structural units, as for example in two-dimensional Kagome and three-dimensional pyrochlore lattices.[2] The *hallmark* of frustration is a large magnetic ground-state degeneracy and consequently the suppression of long-range magnetic ordering. This degeneracy is possibly lifted by structural distortions[3–6] either associated with nonmagnetic instability (bonding requirements, orbital/charge order) or as a consequence of strong magnetoelastic coupling. In the resulting distorted phases, complex noncollinear or partially disordered spin configurations can be observed.[4,7] Recently, this kind of behavior has been reported for $RBaCo_4O_7$ (R, rare earth or Y) cobaltites.[8,9] These compositions belong to a new class of frustrated systems with trigonal symmetry ($P31c$), formed by an alternate stacking of Kagome and triangular layers along the c axis.[10] The unique exchange topology is formed by a network of corner-sharing trigonal bipyramids and triangular clusters.[11] A structural phase transition from trigonal ($P31c$) to orthorhombic symmetry ($Pbn2_1$) has been observed for most compositions, driven by chemical bonding conditions of Ba^{2+} and R^{3+} cations. The temperature of the $P31c \rightarrow Pbn2_1$ phase transition was found to vary from 160 K for $R =$ Lu up to 355 K for $R =$ Ho (Refs. 8,9,12–14). Short-range magnetic correlations, evidenced by diffuse neutron scattering, are drastically enhanced in the orthorhombic phase,[11] but there is still a controversy about the nature of the low-temperature magnetic state. Soda *et al.*[15] reported only short-range correlations in $YBaCo_4O_{7+\delta}$ single crystal and discussed models where the Kagome and triangular layers are fully decoupled, forming spin configurations close to 120°. A similar picture of finite magnetic correlations and decoupled Kagome and triangular spins has been adopted to interpret the neutron diffraction measurements on $LuBaCo_4O_{7+\delta}$ single crystal.[16] On the contrary, long-range magnetic ordering with an intricate magnetic structure has been found for a polycrystalline sample of $YBaCo_4O_7$ below 110 K (Ref. 9). The discrepancy with the single-crystal data is possibly due to the oxygen stoichiometry in the crystal studied by Soda *et al.*,[15] an assumption based on the observation that hyperstoichiometric Y-based and related compositions,[8] which do not undergo the structural transition to the orthorhombic phase, remain short-range ordered. On the other hand, the ^{57}Fe Mossbauer spectra of both $YBaCo_{3.94}Fe_{0.04}O_{7.02}$ and $YBaCo_{3.94}Fe_{0.04}O_{7.80}$ polycrystalline samples collected at 4 K shows well-defined magnetic sextets consisting of two and three components, respectively,[17] a result fully compatible with the presence of long-range magnetic order in both of these compositions.

With the aim to resolve the controversy about the nature of the magnetic state in $YBaCo_4O_7$, we undertook additional neutron-diffraction experiments on single crystal with an oxygen content precisely controlled. Our results are consistent with the scenario of long-range magnetic order, evidenced by the presence of sharp magnetic Bragg peaks. A model for the magnetic structure is proposed from refinements based on a large number of independent reflections. In addition, high-resolution x-ray powder diffraction data clearly indicate that the symmetry of the magnetically ordered state is lowered to monoclinic $P2_1$. The latter observation indicates the strong spin-lattice coupling in the system and its inherent link to the magnetic frustration not fully lifted in the orthorhombic $Pbn2_1$ phase.

II. EXPERIMENTAL

The single crystal of $YBaCo_4O_{7.0}$ was grown by a floating-zone technique in an optical image furnace. A densified rod of the nominal composition was melted in a 20% O_2/Ar atmosphere, and the crystal was grown at 1 mm/h. Because of the high affinity for $YBaCo_4O_7$ to pick up oxygen on cooling,[18,19] an afterheater was used to keep the growing

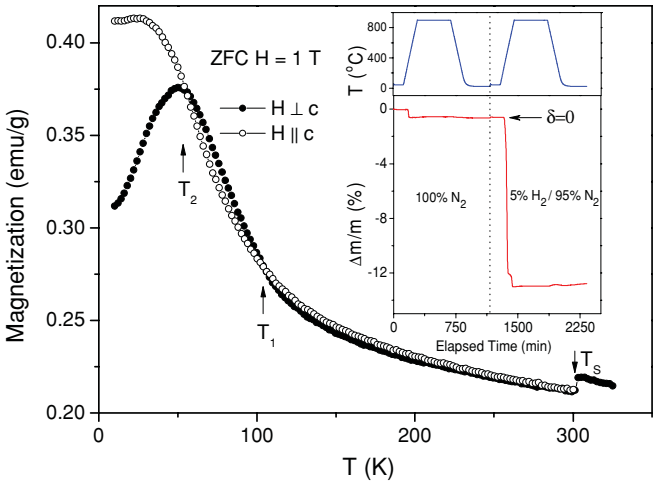

FIG. 1. (Color online) Magnetization of the stoichiometric $YBaCo_4O_7$ single crystal as a function of temperature measured for two directions of the field after cooling in zero field. (Inset) An example of TGA data measured on an as-made $YBaCo_4O_{7+\delta}$ polycrystalline sample.

crystal above 900 °C. After growth was complete, the atmosphere was changed to 99.995% Ar for 24 h and the crystal cooled down to room temperature over 6 h. Oxygen content was verified by thermogravimetric analysis (TGA) of a crushed sample of the crystal. The ceramic samples used for the single-crystal growth and x-ray powder-diffraction experiments were synthesized from high-purity Y_2O_3, $BaCO_3$, and Co_3O_4 reagents by repeated firing in air at 1150 °C. The materials for the x-ray measurements were then treated in nitrogen at 900 °C, resulting in the oxygen content $O_{6.95(5)}$ as determined by thermogravimetry.

An example of the TGA data measured using a Perkin-Elmer TGA-7 instrument on an as-made $YBaCo_4O_{7+\delta}$ polycrystalline sample is shown in the inset of Fig. 1. The sample was heated first in nitrogen to 900 °C and cooled. Then the gas was switched to a 5% H_2/N_2 and heated again. X-ray-diffraction phase analysis of the end point revealed Co metal, Y_2O_3, and BaO. The weight loss was then calculated back to an oxygen content of $O_{7.0}$ for the sample at the beginning of the hydrogen reduction stage. As is clearly seen, this mass is identical to that found when the as-made sample was treated in nitrogen at 900 °C. This mass is preserved on cooling in nitrogen, indicating that the sample does not pick up any oxygen and is stoichiometric at the end of the nitrogen treatment.

Magnetization of the single-crystal sample was measured using a Quantum Design physical properties measurement system for two directions of the magnetic field; parallel and perpendicular to the c axis (Fig. 1). The data do not demonstrate a pronounced magnetic anisotropy but show some divergence below $T_2 \sim 60$ K. The presence of the structural phase transition near $T_S = 300$ K indicated by the steplike change of the magnetization is an additional confirmation of the precise oxygen stoichiometry since this transition is very sensitive to the oxygen content.[8,9]

The neutron-diffraction studies were performed on the PRISMA time-of-flight spectrometer at the ISIS facility, Rutherford Appleton Laboratory (UK), and on the four-circle diffractometer D10 at the ILL (Grenoble, France). For the experiment at ISIS, the single crystal of cylindrical shape (5 mm diameter, 3 mm height) was mounted on an aluminium pin with the [001] vertical axis. For this geometry, scattering in the orthogonal (a^*b^*) reciprocal plane was recorded by rotating the crystal around the [001] axis. Data have been corrected for absorption and normalized to the incoherent scattering of a vanadium standard. The experiment at ILL was done on the same crystal prealigned by using the OrientExpress facility. All data were collected with an incident neutron wavelength of $\lambda = 2.36$ Å by using an 80 mm^2 two-dimensional microstrip detector. Peak integration was performed using the program RACER (ILL) in two steps. First, a library was built by fitting ellipsoidal shapes to a set of strong reflections ($I > 3\sigma$), these shapes were used in a second pass to integrate all reflections. For each data set the list of integrated intensities obtained were corrected for Lorentz factors and normalized to the monitor count. To refine the magnetic structure (propagation vector $\mathbf{k} = 0$), 432 independent reflections were collected at 5 K and 80 K. In addition, the intensity of some selected peaks was measured as a function of temperature (5 K $< T <$ 125 K). The nuclear structure in the paramagnetic phase was refined based on 266 independent reflections measured at 150 K. Refinement of both the nuclear and the magnetic structures was carried out using the FULLPROF program.[20]

A good agreement between the observed and calculated structure factors (RF = 5.95%) in the paramagnetic phase was obtained in the orthorhombic symmetry $Pbn2_1$ ($Pna2_1$ in standard setting) with three types of 120° ferroelastic domains shown in Fig. 2. These domains are expected due to the symmetry relation between the orthorhombic $Pbn2_1$ and hexagonal $P6_3mc$ space groups. The latter is the common supergroup

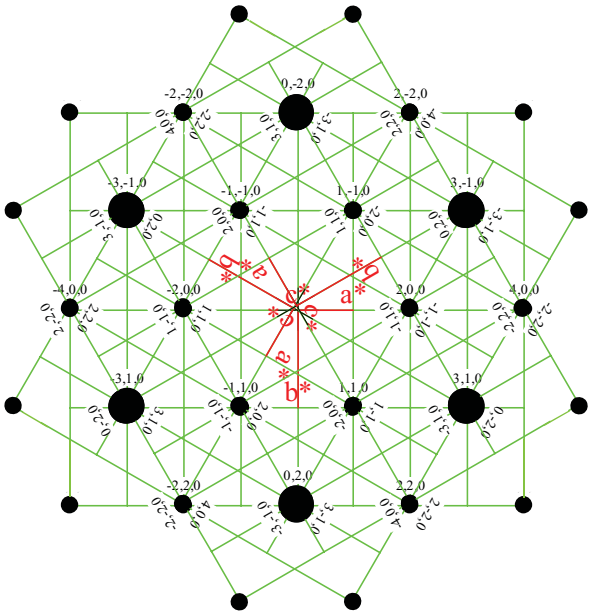

FIG. 2. (Color online) A part of the ($hk0$) reciprocal plane demonstrating superposition of the three types of 120° ferroelastic domains, expected in the case of the orthorhombic $Pna2_1$ symmetry.

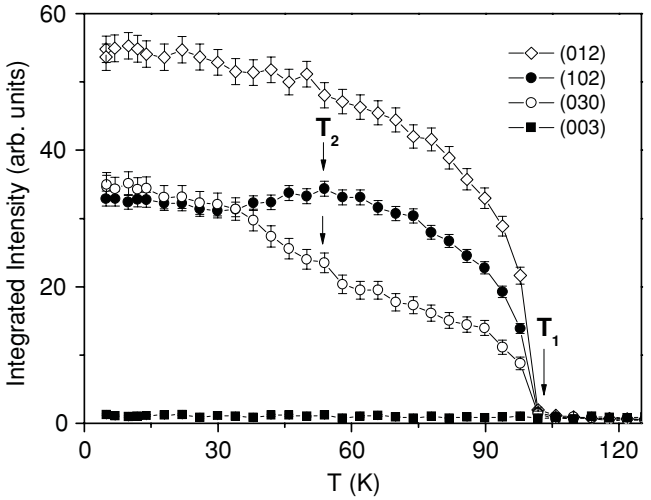

FIG. 3. Integrated intensities of some selected peaks as a function of temperature (error bars correspond to 3σ interval). The indexation relates to the orthorhombic $Pbn2_1$ unit cell with $a \sim 6.30$ Å, $b \sim 10.95$ Å, and $c \sim 10.19$ Å.

of $Pbn2_1$ and $P31c$ and is the parent symmetry which has to be used for classification of domains and displacive modes in the system.[21] Matrix representation of the rotational parts of the three domain generators: {E/000}, {C_{3^+}/000}, and {C_{3^-}/000} were used to introduce the twinning law at the data processing stage. The low-temperature magnetic phases at 5 K and 80 K were refined in monoclinic $P2_1$ space group with six types of domains as discussed in the next section.

High-resolution x-ray powder diffraction data were collected on beamline X16C at the National Synchrotron Light Source (USA). X-rays of wavelength 0.6911 Å were selected by a Si(111) double-crystal monochromator. Samples were mounted on a flat brass plate, and data were collected in the reflection geometry within the temperature interval 10 K $< T <$ 200 K.

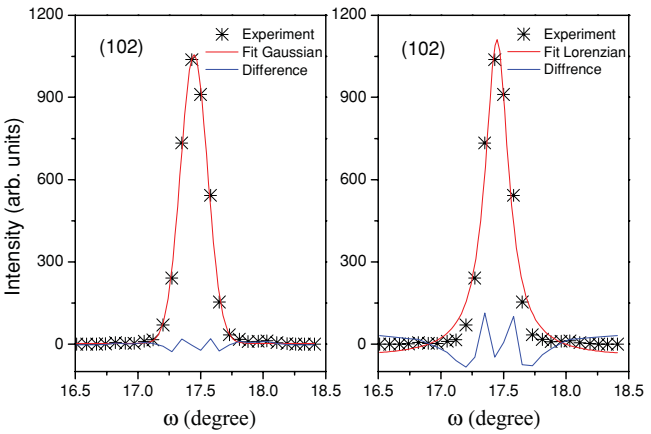

FIG. 4. (Color online) Example of an ω-scan profile for the (102) reflection measured at 5 K on the D10 diffractometer and fitted with a Gaussian (left) and Lorentzian (right) functions. The reflection, forbidden in the $Pbn2_1$ space group, has mainly a magnetic contribution (some small nuclear contribution can exist since it is allowed in $P112_1$).

III. RESULTS AND DISCUSSION

In agreement with the measurements on polycrystalline materials,[9] our single-crystal neutron-diffraction data clearly indicate two successive phase transitions in $YBaCo_4O_7$, which take place at $T_1 \sim 100$ K and $T_2 \sim 60$ K, respectively (Fig. 3); the former has been associated with long-range magnetic ordering (propagation vector $\mathbf{k} = 0$) and the latter with a spin reorientation process.[9] The onset of the long-range ordering does not have any pronounced effect on the magnetization and only slightly changes the slope of the curves (Fig. 1). In the previous single-crystal experiments,[15,16] the magnetic reflections were found to have a Lorentzian shape and a width indicating short-range spin correlations. The authors pointed out that the fundamental discrepancy with the powder-diffraction data[9] could be related to a less accurate estimation of the magnetic component in the powder experiments. In Fig. 4, a ω scan for the (102) reflection measured at 5 K is presented as an example of our single-crystal data. This reflection is forbidden by the n glide plane of the $Pbn2_1$ space group and therefore has mainly a magnetic contribution. In addition, this particular reflection is not affected by the 120° domain structure which can introduce some broadening or asymmetry. The reflection has a perfect Gaussian shape and a width essentially resolution limited, indicating the long-range nature of the magnetic ordering.

A. Symmetry of the magnetically ordered state

The high-resolution x-ray powder diffraction reveals that magnetic ordering is accompanied by structural distortions that reduce the crystal symmetry down to monoclinic (Fig. 5), producing a clear splitting of some of the nuclear reflections below $T_1 \sim 100$ K. The systematic splitting of the $(hk0)$ reflections and the absence of splitting for the $(h0l)$,$(0kl)$ reflections indicate a unit-cell with c as unique axis and γ as the monoclinic angle (Fig. 5, inset). For simplicity, this nonconventional setting will be used to describe the unit-cell rather than transforming the coordinates to the conventional

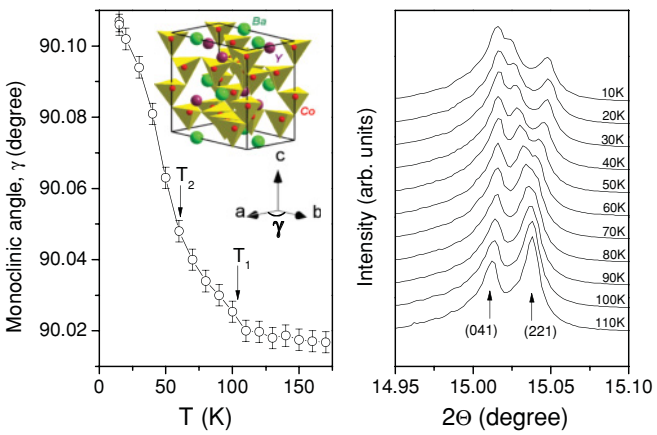

FIG. 5. (Color online) (Left) Monoclinic angle as a function of temperature. The inset shows the orthorhombic unit cell and the angle γ which deviates from 90° in the monoclinic phase. (Right) A part of the x-ray-powder-diffraction patterns collected at different temperatures and demonstrating the splitting of the (221) reflection below $T_1 \sim 100$ K.

TABLE I. Irreducible representations of $Pbn2_1$ space group associated with wave vector $\mathbf{k} = 0$.

Irrep	$\{1\|000\}$	$\{m_{yz}\|\frac{1}{2}\frac{1}{2}0\}$	$\{m_{xz}\|\frac{1}{2}\frac{1}{2}\frac{1}{2}\}$	$\{2_z\|00\frac{1}{2}\}$
Γ_1	1	1	1	1
Γ_2	1	−1	−1	1
Γ_3	1	1	−1	−1
Γ_4	1	−1	1	−1

cell. The temperature dependence of γ is plotted in Fig. 5 (left). Above T_1, the small deviation of γ from 90° is caused by anisotropic peak broadening which often precedes magnetostructural phase transitions.[22] The broadening is known to be due to the presence of anisotropic microstrains which locally break the symmetry but have a random noncooperative character (static fluctuations) and do not change the overall symmetry.[23] In fact, above T_1, refinements with monoclinic symmetry do not improve what is obtained with orthorhombic symmetry, indicating that the structural transition coincides with the magnetic one.

The change of the unit-cell metric at the magnetic transition is associated with the e_{xy} component of the strain tensor, which spontaneously appears below T_1. This observation provides crucial information about the magnetic symmetry because a magnetoelastic coupling invariant, linear with respect of e_{xy}, must be present in the Landau expansion of the free energy. Since the bilinear coupling between e_{xy} and the magnetic order parameter, η, is forbidden by time reversal, one must consider coupling terms that involve even powers of the magnetic order parameter(s). Inspection of the irreducible representations (irreps) of the $Pbn2_1$ space group shows that there are four one-dimensional irreps listed in Table I. The strain component e_{xy} transforms according to the Γ_2 representation. It is obvious that only the direct products $\Gamma_1 \otimes \Gamma_2$ or $\Gamma_3 \otimes \Gamma_4 \ni \Gamma_2$ and therefore only coupling invariants of the form $e_{xy}\eta_1\eta_2$ or $e_{xy}\eta_3\eta_4$ are possible. It is alternatively easy to determine by direct inspection of the irreps table that the only way to lose the mirror symmetries while preserving the twofold axis along c, necessary to stabilize this monoclinic symmetry, is to mix either Γ_1 and Γ_2 or Γ_3 and Γ_4. In the former case, the magnetic symmetry is $P112_1$ and in the latter, it is $P112_1'$. The systematic absence of $(0\ 0\ l = 2n + 1)$ magnetic reflections (Fig. 3), is uniquely consistent with a time-reversed 2_1 axis, and thus we can conclude that below T_1, the magnetic ordering has the symmetry of the reducible $\Gamma_3 \oplus \Gamma_4$ order parameter.

B. Model for the magnetic structure

Both Γ_3 and Γ_4 irreps enter three times in the decomposition of the magnetic representation for the 4*a* sites,

$$\Gamma(4a) = 3\Gamma_1 \oplus 3\Gamma_2 \oplus 3\Gamma_3 \oplus 3\Gamma_4,$$

and therefore one needs to consider three sets of orthogonal basis vectors for each representation, which are given in Table II. The admixture of the two irreps (monoclinic symmetry) splits the 4*a* site into two independent orbits, implying that there are no constraints for magnetic moments of the cobalt sites related by the *b* and *n* glide planes of the $Pbn2_1$ space group, and those can be treated as independent variables in the refinement. On the contrary, the sites related by the $2_1'$ screw axis have parallel in-plane (φ_{ix},φ_{iy}) configuration and an antiparallel out-of-plane (φ_{iz}) component.

TABLE II. Atomic components of basis vectors, $\varphi_{i\alpha=x,y,z}$ of Γ_3 and Γ_4 irreducible representations of $Pbn2_1$ space group entering three times ($i = 3$) in the reducible magnetic representation for an atom occupying the 4*a* Wyckoff position.

4*a*		1[a]			2			3			4		
i		1	2	3	1	2	3	1	2	3	1	2	3
Γ_3	φ_{ix}	1	0	0	1	0	0	1	0	0	1	0	0
	φ_{iy}	0	1	0	0	−1	0	0	−1	0	0	1	0
	φ_{iz}	0	0	1	0	0	−1	0	0	1	0	0	−1
Γ_4	φ_{ix}	1	0	0	−1	0	0	−1	0	0	1	0	0
	φ_{iy}	0	1	0	0	1	0	0	1	0	0	1	0
	φ_{iz}	0	0	1	0	0	1	0	0	−1	0	0	−1

[a] (x,y,z); 2, $(-x+\frac{1}{2}, y+\frac{1}{2}, z)$; 3, $(x+\frac{1}{2}, -y+\frac{1}{2}, z+\frac{1}{2})$; 4, $(-x, -y, z+\frac{1}{2})$.

Another symmetry aspect to consider is the orientation domain structure of the magnetically ordered state. Since the phase transition involves a change of crystal class, $mm2 \rightarrow 2$, each domain of the orthorhombic paramagnetic phase (Fig. 2) gives rise to two ferroelastic domains with lattice vectors $(\vec{a}, \vec{b}, \vec{c})$ and $(\vec{a}, -\vec{b}, -\vec{c})$, respectively. Thus, the refinement of the low-temperature phase must involve six domains and eight nonequivalent Co positions. The following strategy for the magnetic structure refinement has been applied: Initially, only planar spin components were allowed to vary (z component was fixed to zero), in the light of results obtained previously on a polycrystalline sample.[9] Given the large number of variables, we have imposed the additional constraint, not derived from symmetry, that all sites in the Kagome sublattice on one hand and in the triangular sublattice on the other, have the same moment magnitudes. These simplifications, in combination with the symmetry constraints discussed above, lead to 10 independent variables. The refinement converged quickly to a spin configuration equivalent to that proposed from the powder-diffraction data.[9] In the second step, the z components were allowed to vary, with the symmetry constraint discussed previously. The refinement included 16 magnetic parameters (98 in total) and converged with a good final agreement between calculated and measured integrated intensities (Fig. 6) and physically reasonable domain populations. The resulting magnetic structure is shown in Fig. 7 and the refined parameters are given in Table III . We note that an attempt to refine the magnitude of the eight spins independently was not satisfactory, most parameters becoming strongly correlated, suggesting that the best model must be obtained with the aforementioned restriction on the magnitude of the moments.

The magnetic model is very similar to that obtained from the powder-diffraction experiment. The antiferromagnetic ordering in the triangular sublattice is practically identical in both models and no z component for these spins was found from the single-crystal data. However, the spins in the Kagome layers show deviations from the planar structure not initially detected in the powder measurements, with the largest angle ∼40° (Fig. 7, Table III).

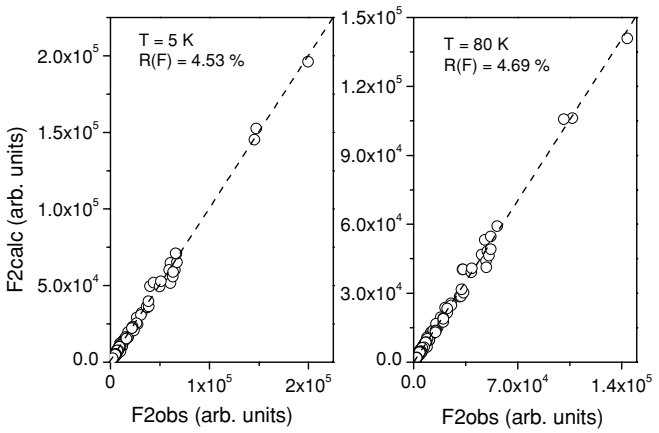

FIG. 6. Experimental structure factors vs calculated ones for the refinement of the data collected at different temperatures (D10 data).

From previous structural work[21] it has been established that the tetrahedra in the Kagome layers make a complex tilt pattern in the orthorhombic phase. These tetrahedral tilts are not rigid modes of the structure and occur with relatively large polyhedral distortions which can essentially modify the local anisotropy of the corresponding Co sites. It appears that the spin configuration with a sizable z component for certain sites is due to this local anisotropy. The average values of the moments in the triangular and Kagome lattices are 2.62(9) and 1.88(6) μ_B, respectively, considerably smaller than the expected spin contribution of 3.25 μ_B for a Co ion with an average +2.25 oxidation state. This suggests that a fraction of the moment remains disordered at low temperature. Additional neutron diffraction data to probe a full two-dimensional section of reciprocal space (Fig. 8) show that indeed diffuse scattering persists down to 2 K.

The data collected at 80 K have been refined using the same strategy. The magnetic structure is shown in Fig. 7 and the refined parameters are listed in Table III. The model suggests a spin reorientation process which has been discussed previously[9] based on competing in-plane and out-of-plane exchange interactions. The transformation from the 5 K structure mainly affects the Kagome sublattice and does not change the magnetic $P112'_1$ symmetry. Thus, the results for the oxygen stoichiometric single crystal are consistent with the powder-diffraction data obtained for the same composition.[9]

The magnetic structures refined here are obtained with less constraints than the powder data and based on many independent reflections. They make it possible to confirm that the model proposed in the previous single-crystal study,[15] where 120° spin configurations were assumed for both Kagome and triangular sublattices is not valid for stoichiometric samples. It is likely that the oxygen content, which can vary largely in these materials, is the cause of such large discrepancy between experimental results.

Also, it is important to note that the model presented produces a small ferromagnetic moment 0.08(6) μ_B per Co ion in the (ab) plane. This value is not statistically significant but the monoclinic symmetry allows for an in-plane ferromagnetic component and, indeed, recently, Izquierdo *et al.*[24] observed it in their low-temperature magnetization study. This result allows us to postulate that the ferromagnetic moment found in

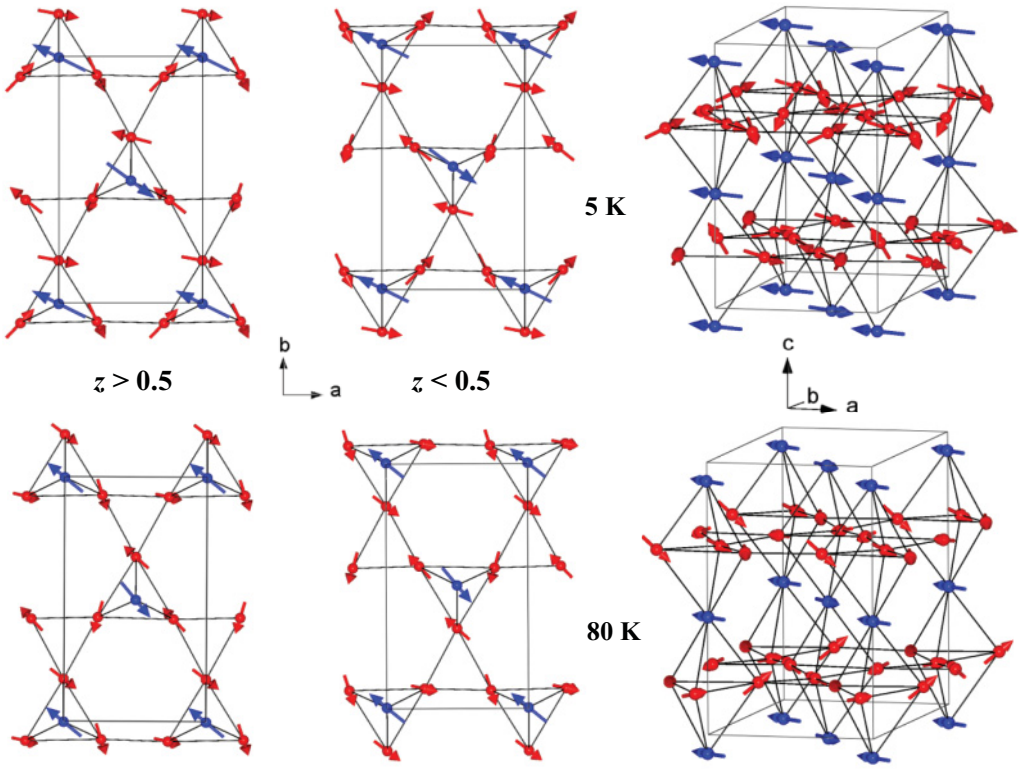

FIG. 7. (Color online) Schematic representation of the magnetic structure of $YBaCo_4O_7$ at different temperatures. The spins in triangular and Kagome sublattices are presented as large (blue) and small (red) arrows, respectively.

TABLE III. Magnetic structure parameters refined in spherical coordinates (M, value of moment; Φ, angle with the x axis; Θ, angle with the z axis) at different temperatures. Coordinates for Co ions are given as they were refined in the $Pbn2_1$ space group at 150 K. Domain fractions at $T = 5$ K and 80 K are: 0.34(1), 0.18(1), 0.11(1), 0.10(2), 0.19(2), 0.08(3) and 0.36(1), 0.18(1), 0.11(1), 0.11(2), 0.16(2), 0.08(3), respectively.

Spherical components	M (μ_B)		Φ (°)		Θ (°)	
Coordinates of Co atom	5 K	80 K	5 K	80 K	5 K	80 K
−0.001(4), −0.004(4), 0.931(3)	2.62(9)	2.04(8)	153(9)	140(7)	90(—)[a]	90(—)[a]
0.001(4), 0.004(4), 0.431(3)	2.62(9)	2.04(8)	153(9)	140(7)	90(—)[a]	90(—)[a]
0.501(4), 0.496(4), 0.931(3)	2.62(9)	2.04(8)	153(9)	140(7)	90(—)[a]	90(—)[a]
0.499(4), 0.504(4), 0.431(3)	2.62(9)	2.04(8)	153(9)	140(7)	90(—)[a]	90(—)[a]
−0.002(3), 0.172(3), 0.672(4)	1.88(6)	1.50(7)	−11(19)	323(14)	103(9)	102(13)
0.002(3), −0.172(3), 0.172(4)	1.88(6)	1.50(7)	−11(19)	323(14)	77(9)	78(13)
0.502(3), 0.672(3), 0.672(4)	1.88(6)	1.50(7)	−195(20)	137(9)	104(8)	101(13)
0.498(3), 0.328(3), 0.172(4)	1.88(6)	1.50(7)	−195(20)	137(9)	76(8)	79(13)
0.768(3), 0.418(2), 0.686(3)	1.88(6)	1.50(7)	141(14)	133(14)	104(6)	108(8)
0.232(3), 0.582(2), 0.186(3)	1.88(6)	1.50(7)	141(14)	133(14)	76(6)	72(8)
−0.268(3), −0.082(2), 0.686(3)	1.88(6)	1.50(7)	46(18)	348(9)	71(8)	128(12)
0.268(3), 0.082(2), 0.186(3)	1.88(6)	1.50(7)	46(18)	348(9)	109(8)	52(12)
0.264(3), 0.925(2), 0.681(3)	1.88(6)	1.50(7)	−65(15)	288(14)	116(6)	104(5)
−0.264(3), −0.925(2), 0.181(3)	1.88(6)	1.50(7)	−65(15)	288(14)	64(6)	76(5)
0.236(3), 0.425(2), 0.681(3)	1.88(6)	1.50(7)	252(19)	254(9)	135(9)	81(9)
0.764(3), −0.425(2), 0.181(3)	1.88(6)	1.50(7)	252(19)	254(9)	45(9)	99(9)

[a]Variation of these parameters resulted in their small oscillations, within 2°–3° interval near $\Theta = 90°$, indicating that there is no detectable z component in the triangular lattice and therefore in the final refinement these parameters were fixed.

$Ca_{1-x}R_xBa(Co/Fe)_4O_7$ must arise from a similar noncollinear spin arrangement rather than from the simple ferrimagnetic ordering with antiparallel Kagome and triangular sublattices, proposed in Refs. 25–27. This assumption is in agreement with the recent neutron diffraction study of $CaBaCo_4O_7$, where a complex $\mathbf{k} = 0$ magnetic structure with noncollinear spin ordering in both triangular and Kagome sublattices has been found.[28]

Finally, it should be pointed out that the magnetic point group $2'$ allows a linear magnetoelectric coupling and is consistent with a presence of spontaneous electrical polarization along the z axis. Thus, the RBa(Co/Fe)$_4$O$_7$ compositions can demonstrate multiferroic/magnetoelectric properties since the necessary symmetry conditions are fulfilled. For the existence of a linear magnetoelectric effect as well as a spontaneous magnetization, the magnetic propagation vector $\mathbf{k} = 0$ is the essential symmetry condition. The spin configurations with this propagation vector found in the $YBaCo_4O_7$ and in the $CaBaCo_4O_7$ (Ref. 28) compositions are apparently the typical situation for this class of materials since magnetic reflections indexed by $\mathbf{k} = 0$ were also observed in $TmBaCo_4O_7$ (Ref. 29) and $YbBaCo_4O_7$ (Ref. 8). This fact can be quantitatively understood based on a simple mean-field consideration. The mean-field ordered states for the prototype hexagonal and trigonal structures have been recently studied in Ref. 30. In these high-symmetry cases, the propagation vector at the K point of symmetry ($\mathbf{k} = \frac{1}{3},\frac{1}{3},0$) yields the lowest energy for a large part of the phase diagram reflecting stability of different magnetic phases as a function of relative strengths of the nonequivalent exchange interactions in the system. However, the energy of the ordered state with $\mathbf{k} = (\frac{1}{2},0,0)$ (M point of symmetry) is always in competition (energy difference ~1%). Although, this state never becomes lowest in energy for the trigonal lattices, it does when the threefold symmetry is broken. The ordered state with $\mathbf{k} = \frac{1}{3},\frac{1}{3},0$ is unstable with respect to symmetry lowering and selection of the $\mathbf{k} = \frac{1}{2},0,0$ wave vector takes place even for small modifications of the exchange parameters, as is illustrated in Fig. 9 for the simplest case of two nonequivalent in-plane interactions with broken threefold symmetry. Since the orthorhombic space group $Pbn2_1$ is an isotropy subgroup of the $P6_3mc$ associated with the M-reciprocal point, the expected magnetic propagation

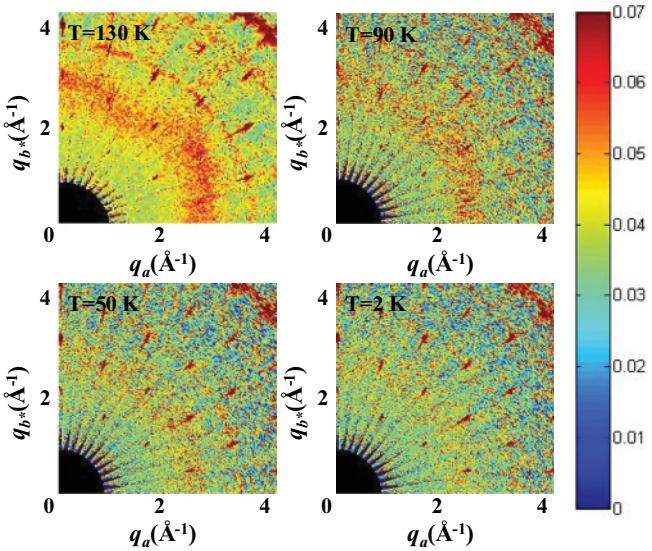

FIG. 8. (Color online) Neutron scattering cross sections measured in the (ab) plane at different temperatures (PRISMA data).

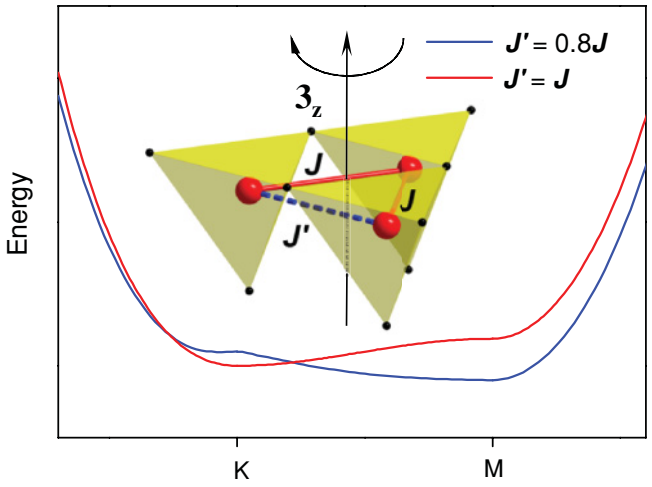

FIG. 9. (Color online) Dispersion relations for low-energy mean-field ordered states in the case of equivalent ($J = J'$; threefold symmetry is preserved) and two nonequivalent ($J \neq J'$; threefold symmetry is broken) exchange parameters in the system (see Ref. 30 for details of the mean-field approach).

vector is $\mathbf{k} = 0$ in terms of the orthorhombic (monoclinic)[31] cell. It should be pointed out that a comprehensive analysis of all possible mean-field ordered states and their stability conditions for the monoclinic structure is an extremely difficult task because of the large number of nonequivalent exchange parameters.

The thermodynamics of the phase transitions involving coupled order parameters has been discussed in a number of works.[32–35] The relevant case implies two one-dimensional order parameters (noted η_3 and η_4 to follow the labeling of the irreps) with biquadratic coupling. The Landau free energy can be written as

$$F(\eta_3,\eta_4) = \frac{\alpha_1}{2}\eta_3^2 + \frac{\alpha_2}{4}\eta_3^4 + \cdots + \frac{\beta_1}{2}\eta_4^2 + \frac{\beta_2}{4}\eta_4^4 + \cdots + \delta\eta_3^2\eta_4^2, \quad (1)$$

where $\alpha_{1,2}$, $\beta_{1,2}$, and δ are coefficients of the expansion. The integrity basis of $F(\eta_3,\eta_4)$ is formed by the two square invariants η_3^2, η_4^2 and, thus, the minimal degree to which the expansion (1) has to be truncated to fully describe the set of symmetry distinct phases is the fourth degree.[34,35] However, in this case the transition from the high symmetry phase to the phase with $\eta_3 \neq 0$ and $\eta_4 \neq 0$ can only take place in a single point of the phase diagram. A more realistic phase diagram, where these phases are separated by a first-order transition line, can be obtained by including a six-degree term in $F(\eta_3,\eta_4)$ for at least one of the order parameters. A comprehensive review of this case as well as the case of the symmetric six-degree expansion can be found in Refs. 34 and 35. However, the isostructural phase transition observed in $YBaCo_4O_7$ does not appear either asymmetric or symmetric six-degree expansion (1). Nevertheless, it is straightforward to show that eight-degree asymmetric expansion can stabilize two distinct thermodynamic phases with $\eta_3 \neq 0$ and $\eta_4 \neq 0$. Minimization of (1) in respect of η_4 gives the equilibrium value for this order parameter:

$$\eta_4^2 = -\frac{\beta_1 + 2\delta\eta_3^2}{\beta_2}. \quad (2)$$

Substituting this expression in the $F(\eta_3,\eta_4)$ truncated at eight-degree with respect to η_3 gives, with some renormalized polynomial coefficients, a well-studied case of a single one-dimensional order parameter. For this case it has been shown[34,35] that inclusion of invariants with the highest degree $2m$ results in $m/2$ stable low-temperature phases having identical symmetry. Thus, taking into account the expression (2), the asymmetric eight-degree expansion of the $F(\eta_3,\eta_4)$ should split the phase space where both components of the reducible $\Gamma_3 \oplus \Gamma_4$ order parameter are not zero into two distinct regions separated by the discontinuous isostructural phase transition. The eight-degree expansion necessary to account for the isostructural transition observed experimentally at T_2 indicates that the energy difference between the two spin configurations is very small. Apparently, this situation is not unique for geometrically frustrated systems, where ground-state degeneracy is lifted by a symmetry lowering. The structural distortions can favor several configurations of initially infinitely degenerated manifold, making the system easily switchable between the different phases. This type of system should be sensitive to external perturbations and may demonstrate rich phase diagrams in the coordinates of thermodynamic variables such as pressure, temperature, and concentration.

IV. CONCLUSIONS

An oxygen stoichiometric single crystal of $YBaCo_4O_7$ exhibits long-range magnetic ordering with propagation vector $\mathbf{k} = 0$ below $T_1 \sim 100$ K. The magnetic ordering breaks the crystal symmetry $Pbn2_1$ to monoclinic symmetry $P112_1$, which has been observed by high-resolution x-ray diffraction. At $T_2 \sim 60$ K, another magnetic phase transition takes place, corresponding to a spin reorientation process and with no additional symmetry breaking. In both magnetic phases (above and below T_2), spins in the triangular sublattice are antiferromagnetically aligned in the (ab) plane with no detectable z component. On the contrary, spins in the Kagome layers are ordered in a complex noncollinear fashion and deviate from the (ab) plane. The transition at T_2 affects mainly the Kagome sublattice. The average values of spins in the triangular and Kagome layers are 2.62(9) μ_B and 1.88(6) μ_B, respectively, at $T = 5$ K. The reduced values with respect to the expected spin contribution for Co in the +2.25 oxidation state is related, at least partially, to disorder and short-range correlations that persist down to 2 K, as evidenced by diffuse neutron-scattering experiments.

ACKNOWLEDGMENTS

We would like to thank P. Toledano for helpful discussions regarding the Landau theory with coupled order parameters. Work at Argonne supported under Contract No. DE-AC02-06CH11357 by UChicago Argonne, LLC, Operator of Argonne National Laboratory, a US Department of Energy Office of Science Laboratory.

[1]R. Moessner and A. P. Ramirez, Phys. Today **59**, 24 (2006).
[2]J. S. Gardner, M. J. E. Gingras, and J. E. Greedan, Rev. Mod. Phys. **82**, 53 (2010).
[3]O. Tchernyshyov, R. Moessner, and S. L. Sondhi, Phys. Rev. Lett. **88**, 067203 (2002).
[4]O. Tchernyshyov, R. Moessner, and S. L. Sondhi, Phys. Rev. B **66**, 064403 (2002).
[5]C. Jia, J. H. Nam, J. S. Kim, and J. H. Han, Phys. Rev. B **71**, 212406 (2005).
[6]T. E. Saunders, and J. T. Chalker, Phys. Rev. B **77**, 214438 (2008).
[7]J. R. Stewart, G. Ehlers, A. S. Wills, S. T. Bramwell, and J. S. Gardner, J. Phys.: Condens. Matter **16**, L321 (2004).
[8]A. Huq, J. F. Mitchell, H. Zheng, L. C. Chapon, P. G. Radaelli, K. S. Knight, and P. W. Stephens, J. Solid State Chem. **179**, 1136 (2006).
[9]L. C. Chapon, P. G. Radaelli, H. Zheng, and J. F. Mitchell, Phys. Rev. B **74**, 172401 (2006).
[10]M. Valldor, and M. Andersson, Solid State Sci. **4**, 923 (2002).
[11]P. Manuel, L. C. Chapon, P. G. Radaelli, H. Zheng, and J. F. Mitchell, Phys. Rev. Lett. **103**, 037202 (2009).
[12]V. Caignaert, A. Maignan, V. Pralong, S. Hebert, and D. Pelloquin, Solid State Sci. **8**, 1160 (2006).
[13]N. Nakayama, T. Mizota, Y. Ueda, A. N. Sokolov, and D. Vasillev, J. Magn. Magn. Mater. **300**, 98 (2006).
[14]A. I. Rykov, Y. Ueda, M. Isobe, N. Nakayama, Yu. T. Pavlyukhin, S. A. Petrov, A. N. Shmakov, V. N. Kriventsov, and A. N. Vasiliev, New J. Phys. **12**, 043035 (2010).
[15]M. Soda, Y. Yasui, T. Moyoshi, M. Sato, N. Igawa, and K. Kakurai, J. Phys. Soc. Jpn. **75**, 054707 (2006).
[16]M. Soda, T. Moyoshi, Y. Yasui, M. Sato, and K. Kakurai, J. Phys. Soc. Jpn. **75**, 084701 (2007).
[17]E. V. Tsipis, J. C. Waerenborgh, M. Avdeev, and V. V. Kharton, J. Solid State Chem. **182**, 640 (2009).
[18]E. V. Tsipis, D. D. Khalyavin, S. V. Shiryaev, K. S. Redkina, and P. Nunez, Mater. Chem. Phys. **92**, 33 (2005).
[19]M. Karppinen, H. Yamauchi, S. Otani, T. Fujita, T. Motohashi, Y. H Huang, M. Valkeapaa, and H. Fjellvag, Chem. Mater. **18**, 490 (2006).
[20]J. Rodriguez Carvajal, Physica B **192**, 55 (1993).
[21]D. D. Khalyavin, L. C. Chapon, P. G. Radaelli, H. Zheng, and J. F. Mitchell, Phys. Rev. B **80**, 144107 (2009).
[22]M. Giot, L. C. Chapon, J. Androulakis, M. A. Green, P. G. Radaelli, and A. Lappas, Phys. Rev. Lett. **99**, 247211 (2007).
[23]M. W. Stephens, J. Appl. Crystallogr. **32**, 281 (1999).
[24]J. L. Izquierdo, J. F. Montoya, A. Gomez, O. Arnache, T. Wolf, and O. Moran, Solid State Commun. **150**, 1951 (2010).
[25]V. Caignaert, V. Pralong, A. Maignan, and B. Raveau, Solid State Commun. **149**, 453 (2009).
[26]B. Raveau, V. Caignaert, V. Pralong, D. Pelloquin, and A. Maignan, Chem. Mater. **20**, 6295 (2008).
[27]V. Pralong, V. Caignaert, A. Maignan, and B. Raveau, J. Mater. Chem. **19**, 8335 (2009).
[28]V. Caignaert, V. Pralong, V. Hardy, C. Ritter, and B. Raveau, Phys. Rev. B **81**, 094417 (2010).
[29]D. D. Khalyavin (unpublished).
[30]D. D. Khalyavin, P. Manuel, J. F. Mitchell, and L. C. Chapon, Phys. Rev. B **82**, 094401 (2010).
[31]The monoclinic $P2_1$ phase preserves the translation symmetry of the orthorhombic $Pbn2_1$ phase.
[32]E. M. Lifshitz, Zh. Eksp. Teor. Fiz. **14**, 353 (1944).
[33]Y. M. Gufan and E. S. Larin, Fiz. Tverd. Tela (Leningrad) **22**, 463 (1980) [Sov. Phys. Solid State **22**, 270 (1980)].
[34]P. Toledano and V. Dmitriev, *Reconstructive Phase Transitions: In Crystals and Quasicrystals* (World Scientific, Singapore, 1996), pp. 105–109.
[35]J. C. Toledano and P. Toledano, *The Landau Theory of Phase Transitions* (World Scientific, Singapore, 1987), pp. 195–198.